

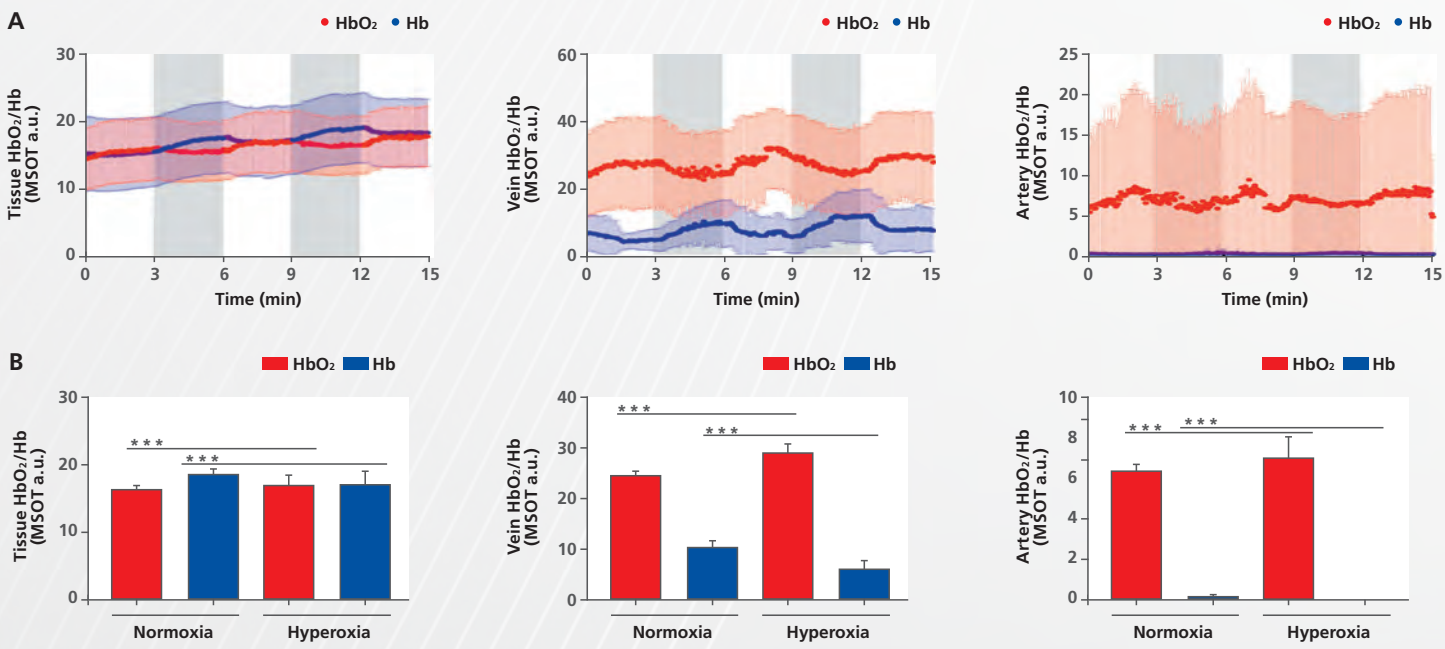
Imaging Hemodynamics in Alzheimer's Disease with Multispectral Optoacoustic Tomography (MSOT)

The brain has a very high demand for oxygen compared to other organs, making tight regulation of cerebral blood flow (CBF) and oxygen delivery critical for brain function. The regional quantification of oxygen saturation (SO_2), brain oxygen extraction fraction (OEF) and, in conjunction with perfusion imaging for CBF, the cerebral metabolic rate of oxygen (CMRO₂) are key measures of brain hemodynamic function. Quantification of these parameters has helped to elucidate brain functional physiology and holds translational potential as a clinical tool for evaluating neurological disorders such as stroke, brain tumors and Alzheimer's disease (AD). AD is associated with vascular dysfunction which is intrinsic to the pathogenesis of the disease. Patients show regional hypoperfusion as well as decreased levels of oxygenated hemoglobin (HbO_2) and tissue

oxygenation. Additionally, capillary dysfunction occurs at an early disease stage. However, the relationships of these features to oxygen transport and metabolism have not yet been investigated as current imaging modalities lack in spatial resolution, sensitivity or penetration depth. In a recent study by Ni R et al. [1], MSOT was exploited to non-invasively derive metrics of tissue oxygenation, extraction and metabolism in mouse brain under different physiological and disease states.

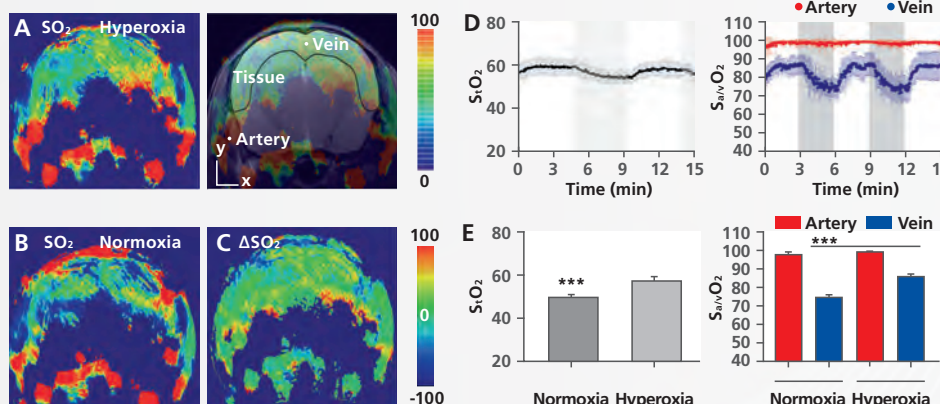
During hyperoxia (0-3, 6-9 and 12-15 min), higher levels of HbO_2 and correspondingly reduced values for Hb have been found in all compartments analyzed (cortical tissue, superior sagittal sinus, middle cerebral artery) when compared to the normoxic (3-6 and 9-12 min) reference (A, B).

FIGURE 1: MSOT imaging of blood oxygenation changes in brain of wild-type mice under oxygen challenge



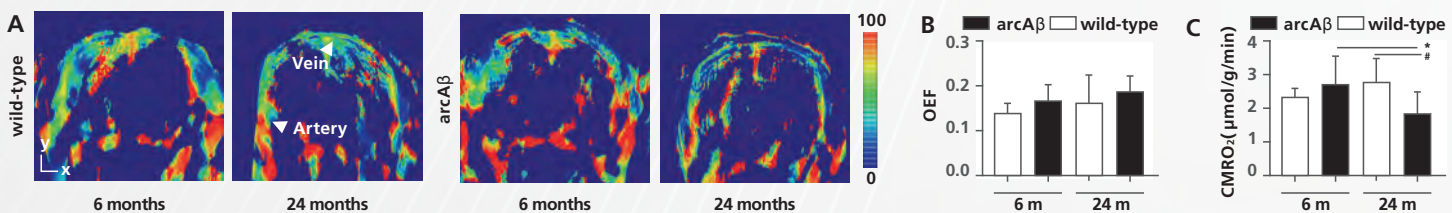
(A) Time course of the HbO_2 and Hb changes in the cortical tissue, vein and artery during normoxic (gray region) and hyperoxic conditions ($n = 10$); (B) Significant difference between HbO_2 and Hb under normoxic and hyperoxic conditions in cortical tissue, vein and artery. *** $p < 0.001$.

Maps of SO_2 and ΔSO_2 were derived from MSOT measurements of Hb and HbO_2 (Figure 2). (A-C) show representative coronal SO_2 and ΔSO_2 maps co-registered with T2-weighted MRI images of a wild-type mouse during oxygen challenge. Arterial oxygen saturation (SaO_2) was estimated in the middle cerebral artery, venous oxygen saturation (SvO_2) in the superior sagittal sinus, and tissue oxygen saturation (StO_2) in cortical tissue. Both StO_2 and SvO_2 with normoxia (3-6 and 9-12 min) and hyperoxia (0-3, 6-9 and 12-15 min) revealed a robust increase in oxygenation during hyperoxia (D), while changes detected in SaO_2 values were smaller. Hyperoxia led to a significant increase in cortical StO_2 and SvO_2 compared to normoxia, whereas the respective arterial value was only non-significantly increased (E).

FIGURE 2: MSOT imaging of brain oxygen saturation in wild-type mice under oxygen challenge

Representative coronal SO₂ map derived from MSOT measurements of Hb and HbO₂ of a brain of a wild-type mouse under (A) hyperoxic and (B) normoxic conditions, approximately Bregma -1.5 ± 0.3 mm; overlaid with T2-weighted magnetic resonance image; (C) ΔSO₂ map shows differences in oxygenation in hyperoxia-normoxia challenge; (D) Cortical StO₂ and Sa/vO₂ derived from MSOT measurements during normoxia (gray region) and hyperoxia in brain of wild-type mice (n = 10); (E) Significant differences between cortical StO₂ and Sa/vO₂ under normoxia and hyperoxia condition. *** p < 0.001.

Lastly, cerebral oxygenation was assessed with MSOT in young and aged arcA β transgenic mice as a model for AD and wild-type controls (Figure 3). OEF and CMRO₂ were determined using the CBF derived from perfusion MRI in 6 months and 24 months old arcA β mice under normoxic conditions (data not shown). (A) shows the SO₂ in the coronal section of the brain of wild-type and arcA β mice at 6 and 24 months of age. MSOT-derived OEF values did not differ between 24 months arcA β and wild-type mice, and 6 months arcA β and wild-type mice (B). Conversely, the MSOT-derived CMRO₂ values were lower in the 24 months arcA β compared to wild-type mice and 6 months arcA β (C). A reduced cortical CBF was found in aged transgenic arcA β mice (data not shown), displaying abundant parenchymal and vascular amyloid deposition. Due to the inability of the vascular system to compensate for the decrease in oxygen delivery by increasing the OEF, CMRO₂ values were found to be significantly decreased, likely putting the tissue under hypoxic stress.

FIGURE 3: In vivo assessment of brain oxygenation in arcA β mice using MSOT

(A) SO₂ maps of arcA β and wild-type mice at 6 and 24 months (coronal view, approximately Bregma -1.5 ± 0.3 mm); (B) Quantification of OEF and (C) CMRO₂ in the brain of arcA β and wild-type mice at 6 months and 24 months of age. OEF does not significantly differ between groups. CMRO₂ is lower in the 24 months arcA β mice compared to wild-type and 6 months arcA β mice. *,# p < 0.05.

Conclusions

Similar to BOLD MRI, MSOT allows for the non-invasive assessment of functional hemodynamic parameters in the brains of mice with chronic neurodegeneration. The investigations revealed that MSOT can sensitively and robustly detect physiological changes in vascular and tissue oxygenation and metabolism with whole brain coverage and high spatial resolution. Metrics of SO₂ could be derived in single feeding and draining vessels and cortical tissue. MSOT can therefore visualize and quantify brain function.

MSOT Imaging Protocol

Acquisition System	Single-Wavelength Image Acquisition/Display Rate	Multispectral Acquisition Wavelengths Used	Analysis Method
MSOT inVision 256-TF small animal scanner	10 Hz	715, 730, 760, 800, 850 nm	model-based tomographic image reconstruction linear regression spectral unmixing

References

[1] Ni R et al.,
Cortical hypoperfusion and reduced cerebral metabolic rate of oxygen in the arcA β mouse model of Alzheimer's disease,
Photoacoustics. 2018 Jun; 10: 38-47.